

The Hall A Beam Line at Jefferson Lab: Present and Future

Jay Benesch and Yves Roblin (2 April 2021 version)

Abstract

The Continuous Electron Beam Accelerator Facility (CEBAF) was built with a thermionic electron source and the three original experimental hall lines reflected this. A few years after beam delivery began a parity violation experiment was approved and two polarimeters were installed in the Hall A beam line without consultation with the accelerator physics group. The beam raster system was placed after the new Compton polarimeter, before one accelerator quadrupole and four quadrupoles in the new Moller polarimeter. It was very difficult to meet experimental requirements on envelope functions and raster shape with this arrangement so a member of the accelerator physics group had a sixth quadrupole installed downstream of the Moller polarimeter. All of the parity experiments in Hall A have been run with this still-unsatisfactory configuration. The MOLLER experiment is predicated on achieving a 2% error on a 32 ppb asymmetry. Beam line changes are required to meet the systematic error budget. This paper documents the existing beam line, an interim change which can be accomplished during a standard annual maintenance down, and the final configuration for MOLLER and subsequent experiments.

Present beam line

Beam envelopes with as-measured emittances at 11 GeV are shown in Figure 1. Full vertical scale is 1 mm; minimum beam pipe ID is 22 mm. All optics work by the first author is done in OptimX (1) and most figures are generated therein.

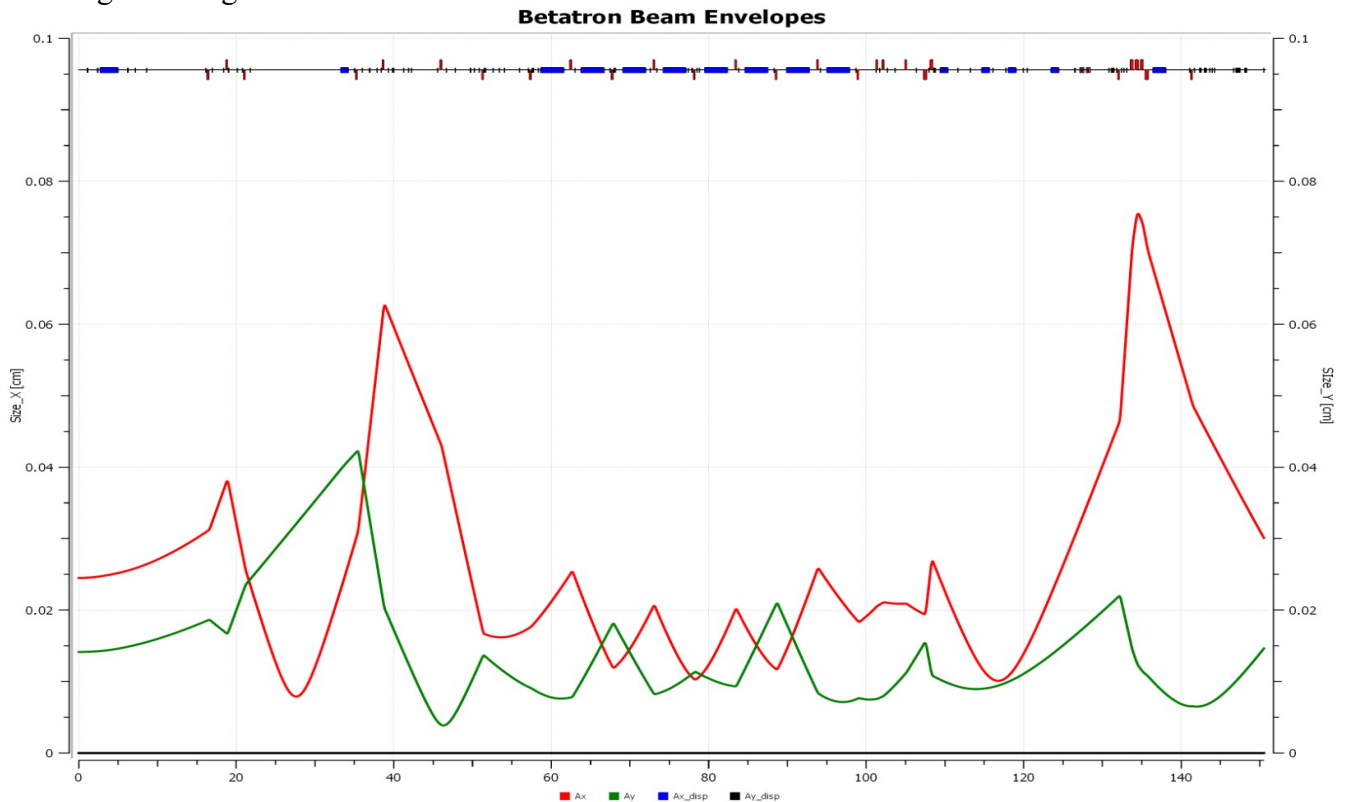


Figure 1. Normal target location is at the right edge of the plot. The horizontal beam size (red) is twice the vertical (green). This is a result of the competing constraints on the beam with inadequate variables.

A 5 mm square raster at the target is standard. The figure below shows the results with the horizontal raster (red) at power supply maximum 50 A and the vertical at 34 A. The raster is driven by a triangle wave at 25 kHz; it suffices to show DC result for those currents. The requirement that 2.5 mm half-response be obtained at 50 A prevents the horizontal and vertical envelopes from being matched in Figure 1 given six quadrupoles between raster and target.

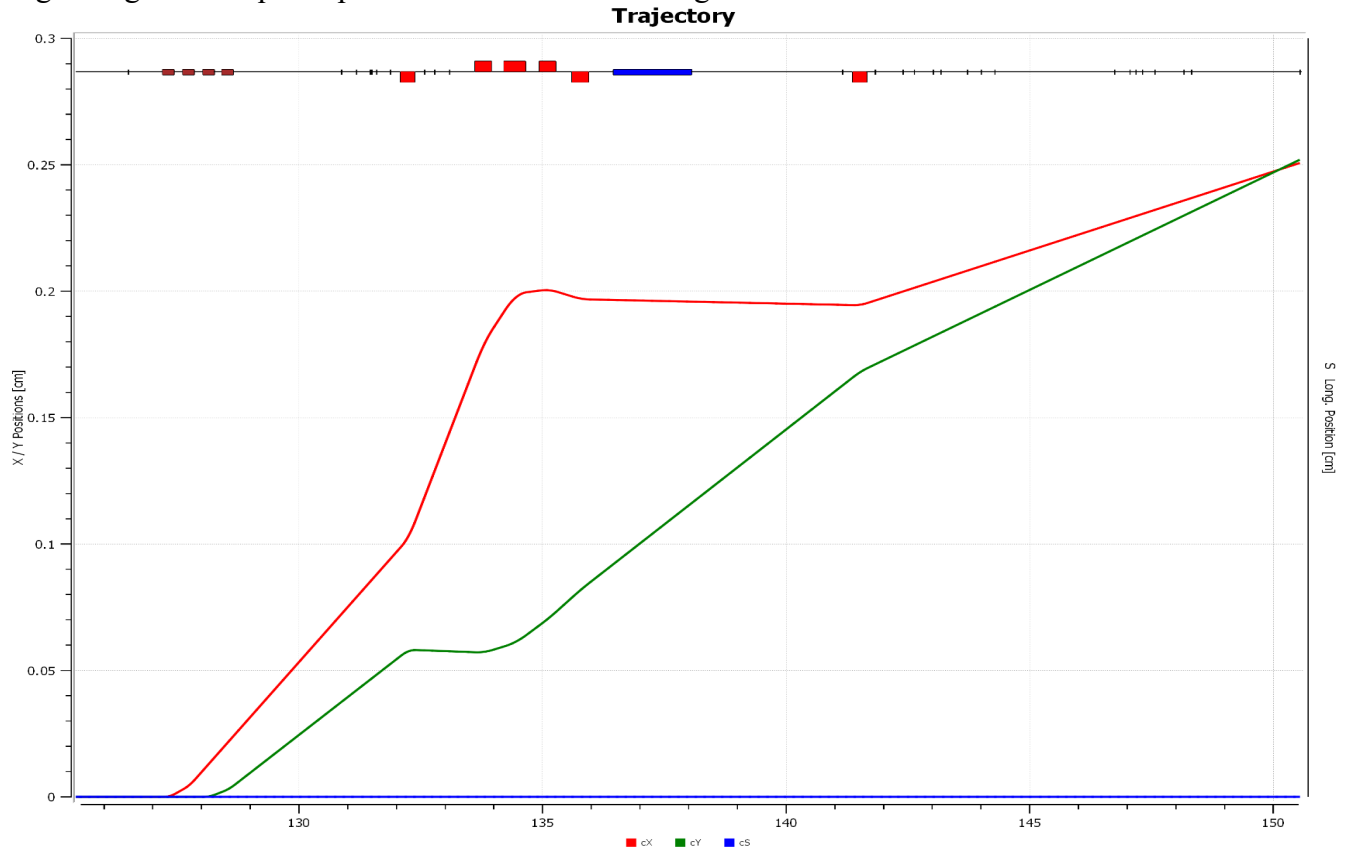


Figure 2. Raster response with subsequent quadrupoles set to provide envelopes in Figure 1. 50 A horizontal and 34 A vertical drive. Note the horizontal scale change from figure 1; this figure shows only the last 25 m to the pivot vs 150.5 m there.

In Figure 2 one seems the four quads of the Moller polarimeter (red) are quite close together and so do not act fully independently as they would with larger drifts between them. Blue is the polarimeter dipole which is energized only when polarization is being measured. Among the requests which are not fulfilled by this optics is the preference for a round spot on the Moller polarimeter iron target foil; the ratio shown in figure 1 is 4:1 x:y. Only the quadrupoles downstream of the Compton polarimeter (four dipoles at S=100-120 m in Figure 1) may be used for final focus and raster adjustment as those before must be used to achieve a 100 micron round spot where the polarized laser beam intersects the electron beam. It is also desirable to have zero derivatives of the envelope (beta) functions at the target so small changes in input betas and alphas do not affect the beam size at the target. One needs to maintain an envelope less than a mm throughout the beam line, even if the input emittances are larger than specified, in order to reduce generating beam halo which will become background in the nuclear physics spectrometers. There are effectively four variables available via the six quadrupoles in Figure 2 and ten parameters which the beam line designer would like to minimize. The problem is over constrained.

CEBAF accelerator physics and operations personnel have contended with this for two decades. The first author began designing alternatives a decade ago but there was no compelling reason to make

changes until the MOLLER (2) experiment was approved. The need for almost an order of magnitude improvement in systematic error over Qweak finally mandated change. The final optics for that experiment, which will remain in Hall A thereafter and be used for all subsequent experiments, is described in what follows.

Parity Experiment requirements

The history of parity violation (PV) experiments is summarized in references 3 and 4. The first CEBAF PV experiment was HAPPEX (5). Table 1 below is taken from (6), the submission to PRL of the latest Jlab parity experiment to complete analysis, PREX-II.

Table 1. Corrections and systematic uncertainties to extract A_{meas} PV listed on the bottom row with its statistical uncertainty.

Correction	Absolute [ppb]	Relative [%]
Beam asymmetry	-60.4 ± 3.0	11.0 ± 0.5
Charge correction	20.7 ± 0.2	3.8 ± 0.0
Beam Polarization	56.8 ± 5.2	10.3 ± 1.0
Target diamond foils	0.7 ± 1.4	0.1 ± 0.3
Spectrometer rescattering	0.0 ± 0.1	0.0 ± 0.0
Inelastic contributions	0.0 ± 0.1	0.0 ± 0.0
Transverse asymmetry	0.0 ± 0.3	0.0 ± 0.1
Detector nonlinearity 0.0 ± 2.7	0.0 ± 0.5	
Angle determination	0.0 ± 3.5	0.0 ± 0.6
Acceptance function	0.0 ± 2.9	0.0 ± 0.5
Total correction	17.7 ± 8.2	3.2 ± 1.5
A_{meas} PV and statistical error	550 ± 16	100.0 ± 2.9

The Qweak final results (6): Asymmetry- 226.5 ± 7.3 ppb (stat) ± 5.8 ppb (syst); total uncertainty 9.3 ppb or 4.1%. Systematic error was 2.6% so even if beam time had been doubled to lower statistical error, total error would have been 3.4%. This is the smallest asymmetry yet measured at CEBAF. The adjustment to the measured result was not couched in the same terms as used in Table 1, see the paper. Per the MOLLER final conceptual design report (8), the measured asymmetry expected is ~ 32 ppb.

Table 2: Expected fractional errors are (Table 3 of CDR, Ref 8, page 22 of pdf)

Error Source	Fractional Error (%)
Statistical	2.1
Absolute Norm. of the Kinematic Factor	0.5
Beam (second order)	0.4
Beam polarization	0.4
$e + p(+\gamma) \rightarrow e + X(+\gamma)$	0.4
Beam (position, angle, energy)	0.4
Beam (intensity)	0.3
$e + p(+\gamma) \rightarrow e + p(+\gamma)$	0.3
$\gamma(*) + p \rightarrow (\pi, \mu, K) + X$	0.3
Transverse polarization	0.2
Neutral background (soft photons, neutrons)	0.1
Linearity	0.1
Total systematic	1.1

The fractional systematic error required by MOLLER is 40% of that achieved by Qweak and the absolute systematic error needed is 0.35 ppb versus 5.8 ppb for Qweak, a factor of sixteen. The CEBAF injector is being rebuilt with a higher kinetic energy source (less space charge effect) and focusing elements with one tenth the focusing variation across the full beam width (6σ) than was the case for the experiments performed to date. This is done to reduce helicity correlated beam parameters so fast and slow reversals will cancel asymmetries. It must be possible to measure most of the parameters in Table 2 in the Injector and Hall A and feed back as possible to minimize their effects integrated over the course of the expected four years (100 weeks beam time) of operation. The Hall A beam line must also be rebuilt and diagnostics added to make possible (if still unlikely) the required fractional errors. The 2020 MOLLER Conceptual Design Report (8) ties these requirements to hardware implementation. The evolution of the CEBAF injector is dealt with in (9). The remainder of this paper will address the changes in the Hall A beam line. An element list including magnets, diagnostics, drifts and some vacuum equipment follows. As is standard in accelerator physics codes, diagnostics and steering magnets are represented as points. Drifts, dipoles, quadrupoles and raster magnets are the only elements with finite length.

Basic constraints

The principal constraints are the length of the MOLLER experiment and the diameter of Hall A. In 2009, when the first author first designed an altered beam line for Hall A in concert with the first MOLLER proposal to the Jefferson Lab Physics Advisory Committee, the center of the LH2 target was to be 6 m upstream of the center of the hall, the normal pivot. The only way to meet all the constraints was to use the Moller polarimeter quads as part of the production beam focusing elements. Since it was also necessary to move the raster downstream of all focusing elements, this required moving the entire polarimeter upstream.

In 2018 a detailed cost analysis of the beamline rework was done. The cost to move the polarimeter upstream was sufficiently large that the JLab Associate Director for Nuclear Physics required that it remain fixed. The MOLLER experiment target and detector system had evolved by this time so the target center was now 4.5 m from the center of the hall rather than 6 m. This additional beamline space downstream of the polarimeter for diagnostics and the upstream space made available by fixing the polarimeter allowed the production beam transport system to change. The six polarimeter magnets would be energized only during polarization measurements and degaussed thereafter. A triplet of 2.85 cm ID accelerator magnets with spacing about 220 cm would be used to re-focus the round beam coming out of the Compton polarimeter. The raster would follow the accelerator quads; its response through the degaussed polarimeter would be the same as through a drift.

One skilled in the art sees in Figure 1 that the nominal 12 GeV optics has two dispersion peaks; these are about 1.5 m. This was done to reduce the energy spread generated by synchrotron radiation in the arc. The collaboration requests that there be one dispersion peak of 4 m, as in all previous parity experiments, to improve resolution of the on-line energy monitor. Accordingly, the strengths of the quads upstream of the reworked region will be changed. No elements will be moved, only the current supplied will change. The resulting optics will be shown in a later section.

Element list

N is the element number within the entire Hall A beam line. Name is that used by the EPICS control system. S is the distance along the beam path from the start of the Hall A beam line to the end of the specified element. L is the element length, steel-only for magnets, not effective length. BCM is a cavity-based Beam Current Monitor. Unser is different type of current monitor, used to calibrate the others. This was also generated in OptimX (1).

N	Name	description	S[cm]	L[cm]	B[kG]	G[kG/cm]
235	GMCP1P04	end of Compton polarimeter	12453.5	0		
236	oD4000	drift	12470.8	17.27		
237	iIHV1H00	gate valve	12470.8	0	0	0
238	oD4001	drift	12480.5	9.68		
239	iIPM1H01	short stripline BPM center	12480.5	0	0	0
240	oD4002	drift	12495.5	15.02		
241	qMQK1H01	quadrupole	12526	30.48	0	2.63
242	oD4003	drift	12545.1	19.08		
243	kMBC1H01H	horizontal corrector center	12545.1	1.00E-06	0	0
244	oD4004	drift	12564.7	19.61		
245	kMBC1H01V	vertical corrector center	12564.7	1.00E-06	0	0
246	oD5000	drift	12583.6	18.95		
247	iITV1H01	viewer	12583.6	0	0	0
248	oD5001	drift	12698.8	115.21		
249	iIPM1H02	short stripline BPM center	12698.8	0	0	0
250	oD4009	drift	12711.3	12.48		
251	qMQR1H02	quadrupole	12746.9	35.56	0	-3.4
252	oD4010	drift	12762.9	16.01		
253	kMBC1H02H	horizontal corrector center	12762.9	1.00E-06	0	0
254	oD4011	drift	12782.5	19.61		
255	kMBC1H02V	vertical corrector center	12782.5	1.00E-06	0	0
256	oD5002	drift	12817.7	35.19		
257	iIBC1H02A	Cavity Beam Current Monitor BCM	12817.7	0	0	0
258	oD5003	drift	12852.5	34.8		
259	iIUN1H02	Unser Current Monitor	12852.5	0	0	0
260	oD5004	drift	12887.3	34.8		
261	iIBC1H02B	BCM	12887.3	0	0	0
262	oD5005	drift	12917.2	29.89		
263	iIPM1H03	short stripline BPM center	12917.2	0	0	0
264	od4013	drift	12932.2	15.02		
265	qMQK1H03	quadrupole	12962.7	30.48	0	2.27
266	oD4014	drift	12981.8	19.08		
267	kMBC1H03H	horizontal corrector center	12981.8	1.00E-06	0	0
268	oD4015	drift	13001.4	19.61		
269	kMBC1H03V	vertical corrector center	13001.4	1.00E-06	0	0
270	oD4016	drift	13018	16.6		
271	krastX	horizontal raster coil	13043	25	0.23	0
272	oD4017	drift	13058.5	15.52		
273	krastY	vertical raster coil	13083.5	25	0.24	0
274	oD5006	drift	13114.4	30.91		

N	Name	description	S[cm]	L[cm]	B[kG]	G[kG/cm]
275	iIPM1H04	20 cm BPM center	13114.4	0	0	0
276	oD4019	drift	13130.8	16.41		
277	iIHA1H04	wire scanner	13130.8	0	0	0
278	oD4020	drift	13140.6	9.85		
279	iIHV1H04	gate valve	13140.6	0	0	0
280	oD5007	drift	13163.6	22.92		
281	iIPM1H04AX	nA cavity BPM X	13163.6	0	0	0
282	oD5008	drift	13193.1	29.53		
283	iIPM1H04AY	nA cavity BPM Y	13193.1	0	0	0
284	oD4023	drift	13220.8	27.76		
285	iIBC1H04A	cavity BCM	13220.8	0	0	0
286	oD5009	drift	13240	19.11		
287	iIPM1H05	short stripline BPM center	13240	0	0	0
288	oD5010	drift	13281.2	41.29		
289	iIMollTar	Moller polarimeter target foil	13281.2	0	0	0
290	oD4026	drift	13360.8	79.6		
291	qMQO1H06	Moller polarimeter quadrupole 1	13397.1	36.22	0	0
292	oD4027	drift	13421.8	24.71		
293	qMQM1H07	Moller polarimeter quadrupole 2	13466.8	45.05	0	0
294	oD4028	drift	13494	27.2		
295	qMQO1H08	Moller polarimeter quadrupole 3	13530.2	36.22	0	0
296	oD4029	drift	13560	29.78		
297	qMQO1H09	Moller polarimeter quadrupole 4	13596.2	36.22	0	0
298	oD4030	drift	13642	45.71		
299	bMMA1H10	Moller polarimeter dipole	13803.8	161.8	0	0
300	oD5011	drift	14128.2	324.41		
301	iIPM1H11	20 cm BPM center	14128.2	0	0	0
302	oD5012	drift	14144.6	16.41		
303	iIHV1H11	vacuum valve	14144.6	0	0	0
304	oD4033	drift	14152.6	8		
305	iIHA1H11	wire scanner	14152.6	0	0	0
306	oD5013	drift	14188.4	35.85		
307	iIBC1H12A	electrically isolated cavity BCM	14188.4	0	0	0
308	oD5014	drift	14215.8	27.41		
309	iIBC1H12B	electrically isolated cavity BCM	14215.8	0	0	0
310	oD5015	drift	14243.7	27.87		
311	iIBC1H12C	electrically isolated cavity BCM	14243.7	0	0	0
312	oD5016	drift	14288.4	44.7		
313	iIPM1H13AX	nA cavity BPM X	14288.4	0	0	0
314	oD4038	drift	14317.9	29.53		
315	iIPM1H13AY	nA cavity BPM Y	14317.9	0	0	0
316	oD5017	drift	14347.5	29.53		
317	iIBC1H13	cavity BCM	14347.5	0	0	0
318	oD5018	drift	14378.6	31.11		
319	iIHA1H14	wire scanner	14378.6	0	0	0
320	oD4041	drift	14395	16.41		
321	iIPM1H14	20 cm BPM center	14395	0	0	0
322	oD5019	drift	14427.6	32.66		

N	Name	description	S[cm]	L[cm]	B[kG]	G[kG/cm]
323	iIBC1H15	MPS BCM	14427.6	0	0	0
324	oD4043	drift	14439.4	11.76		
325	iIHV1H15	gate valve	14439.4	0	0	0
326	oD5020	drift	14605.1	165.68		
327	iMOLLER	MOLLER LH2 target center	14605.1	0	0	0
328	oD4045	drift	15055.1	450		
329	iPivot	pivot in center of hall	15055.1	0	0	0
330	oD3025a	drift	15555.1	500		
331	iSolid	future SoLID target location	15555.1	0	0	0
332	oD3025b	drift	17305.1	1750		
333	iDetPlne	MOLLER detector plane	17305.1	0	0	0
334	oD3026	drift	17705.1	400		
335	iHLwall	wall of Hall A	17705.1	0	0	0
336	oD3027	drift	19905.1	2200		
337	iDumpFc	dump face	19905.1	0	0	0

Discussion

During all beam transport except Moller polarimetry, quadrupoles 241, 251 and 265 form a triplet with 219 cm center to center spacing. The central quad is longer and has a different pole shape to provide greater focusing range. Correctors are small steering magnets with ~10 kG-cm capability, bipolar.

BCM is a cavity-based Beam Current Monitor. Unser is different type of current monitor (10). Seven Physics BCMS are present in the beam line, two associated with the Unser (257, 259 Unser, and 261); two associated with cavity position monitors (285, 317) and three in a separate enclosure (307, 309, 311). The last three are electrically isolated from each other and the beam line so the only ground is through the signal cable. The distance between these cavities will provide ~160 dB of cavity to cavity RF signal isolation even without the ceramic break. It is intended that these be the primary current monitors and expected, from Qweak performance, that the error allowance on beam intensity in Table 2 will be met. The BCM/Unser/BCM triplet is isolated from ground but the three are at the same potential. These seven current monitors are calibrated with beam against the Unser multiple times each run. The eighth BCM, 323, is used in the Machine Protection System (MPS). There is one in each of the halls. The sum of the hall MPS BCMS is subtracted from a similar unit at the end of the injector. If the difference is greater than ~1% the MPS system turns off beam at the source and the Operations group works to find the location and cause of the beam loss. The 1% allowance is needed in part because the MPS BCMS are not calibrated with beam against the Unser systems in Halls A and C; there are no Unsers in the Halls B and D lines as their currents are too low to accurately register. The MPS BCMS are tuned to resonance at a fixed temperature (41 C) and maintained there with insulated and heated jackets via a per-BCM temperature feedback system.

Position monitors are four-antenna stripline devices. There are two types in the proposed Hall A line, one with wire antennas (20 cm, present standard) and a shorter version with machined antennas (14 cm, elements 239, 249, 263, 287). The latter is needed to make everything fit. The short machined versions have only been used at low energy in a test beam. The RF engineer responsible for the design states that it should have the same resolution as the older wire design down to 10 nA. For lower current, used in tracking studies to determine Q^2 , position monitors consisting of two cavities sensitive to off-axis position and one to current are used, elements 281/283/285 and 313/315/317. The current signal is used to normalize the output of the position cavities. Position monitors 275 and 321 are 1269

cm apart. The collaboration specified a distance of at least 1000 cm to allow sufficient beam angle resolution. Cavities monitoring low current X positions, 281 and 313, are 1115 cm apart, also exceeding the requirement.

Wire scanners are an invasive diagnostic used to measure beam size via a slow scan of a 25 or 50 micron wire across a low to moderate (25 uA) beam, elements 277, 305 and 319. Three wire scanners allow one to fit a parabola to the X and Y beam sizes to determine beam size at the target center or another location of interest, for instance the Moller polarimeter target.

The Moller polarimeter is comprised of elements 289 through 299. Position monitor 301 is mounted above the downstream end of the polarimeter detector box. Since the latter is at a lower height it is not in the element list. Four quadrupoles are used to deflect and focus the half-energy Moller-scattered electrons into tubes beside the main beam line; they are then deflected downward into the polarimeter detector by the dipole. These elements are shown as having zero field/gradient because they aren't used during production beam transport and will be demagnetized after each measurement. Space has been left in the beam line for air core, iron return correctors atop the back half of the polarimeter detector box. These would provide steering in case beam deflections in the polarimeter quads and dipole are sufficient to move the unscattered beam to an unfortunate location. Conceptual design and preliminary engineering is complete. If installed, they would also be demagnetized after each polarization measurement. The magnetized iron foil target of the polarimeter is moved 30 cm upstream from present location in order to improve detector acceptance at 11 GeV and allow the error to be reduced to the 0.4% needed for Table 2. The Compton polarimeter will also be upgraded; that is not covered in this paper. Transverse polarization fraction can only be measured (and nulled) in the 6 MeV/c region of the injector, using a Mott polarimeter. However, the injector is set up to change polarization from longitudinal to transverse by a well defined 90° rotation so measurement of beam normal spin asymmetries can be made in the hall to provide information on the magnitude of that helicity correlated asymmetry and include its effect in the final result.

Helicity correlated beam position, angle and energy variations must be measured and corrected for numerically and via feedback systems. See Table 2 for error quota. The measurement is done by equipping the position monitors with fast sample and hold cards so helicity dependent signals can be measured within each helicity window. The numerical correction can be derived in two ways: analysis of response to random jitter upstream in the Hall A beam line or small driven responses. A 240 Hz oscillator is switched to one of five devices so driven data can be obtained, generally for a minute per device per hour. The energy variation is provided by small signal input to the drive in one of the South Linac cryomodules. Position variation is provided by two small horizontal and two small vertical correctors in the Hall A beam line arc. The X/Y pairs are separated by enough phase advance that the responses of the BPMs after the quad triplet, e.g. elements 275 and 321, are not degenerate and can be deconvolved. See Figure 5 for coil locations.

In Table 2 Beam (second order) effects are budgeted for an error as large as first order. This is in large part because they cannot be measured on the electron beam, only on the laser before it hits the photocathode.

The raster is placed after all magnetic elements which are powered during production running. The shaped response seen in figure 2 is therefore absent: the response is a straight line. See Figure 6. Only a single set of raster coils can be used on the new beam line due to the MOLLER target position 450 cm upstream of the usual location. For a target at the usual location, the single X coil requires 25% more current than each of the two X coils in Figure 2. The single Y coil requires 80% more current

than each of the two Y coils in Figure 2. For a target at the usual location, the currents needed in the single raster coil of each plane are 77% of those at the MOLLER target center for same raster span. The raster frequency is 25 kHz. A test has been run with the existing raster power supplies which can provide a 60 A zero to peak triangle wave. Equilibrium temperature was measured at 10 A intervals and a parabola fit to the data. The extrapolated temperature at 80 A is 64 C. At 100 A the projected temperature is 84 C. The insulation on the existing coils is polyurethane with nylon overcoat, 130 C continuous rating. The test will be repeated when the requested 100 A zero to peak power supply has been prototyped.

Steering and alignment

The BPMs which will be used for the slow orbit lock are 1H11 and 1H14, elements 275 and 321, which are 1269 cm apart. The distance between 1H14 (321) and the MOLLER detector plane (333) is 2951.5 cm. It follows that angle steering errors are multiplied by 2.3. The detector ring for the elastic scattered electrons has 40 mm radial extent. From Figure 30 of Ref. 8 page 57 (pdf 71), a mm shift in beam location is contraindicated. It follows that angle error exiting the slow orbit lock BPM pair should be 15 μ rad or less. Achieving this will be difficult. The random angle fluctuation at 1 kHz (helicity pair) is required to be 4.7 μ rad per Table 5 of Ref. 8 page 15 (p 29 of pdf). The slow orbit lock is generally run with five seconds between updates. Given the accelerator diagnostic monitoring system update rate of 1 Hz, two second intervals are the best that can be done. *Mention FFB?*
Reference for FFB?

Null collimator and spectrometer transverse offsets (x,y) and angles (pitch, yaw) are difficult to achieve. If all the correctors in the element list are upgraded to MBD, with 18 kG-cm strength, only 0.7 mm vertical offset can be dealt with if pitch and yaw are zero. Horizontal plane has 4 mm capability in this case, which should suffice. The MBD corrector has been modeled in Opera. It appears that the maximum strength may be doubled via new power supplies if the existing water cooling suffices or additional cooling is provided. The wire is 2 mm square and so should take 20 A, versus 10 A maximum now.

The LH2 target is 125 cm long with 127 micron aluminum alloy beam windows. There are solid targets on the same vertical ladder to allow for systematic studies including measurement of the scattering from the windows on the LH2 target. The end of the target is at 145.676 m from the start of the Hall A line; 147 m will be the terminus in figures 3-5 which follow.

MOLLER optics

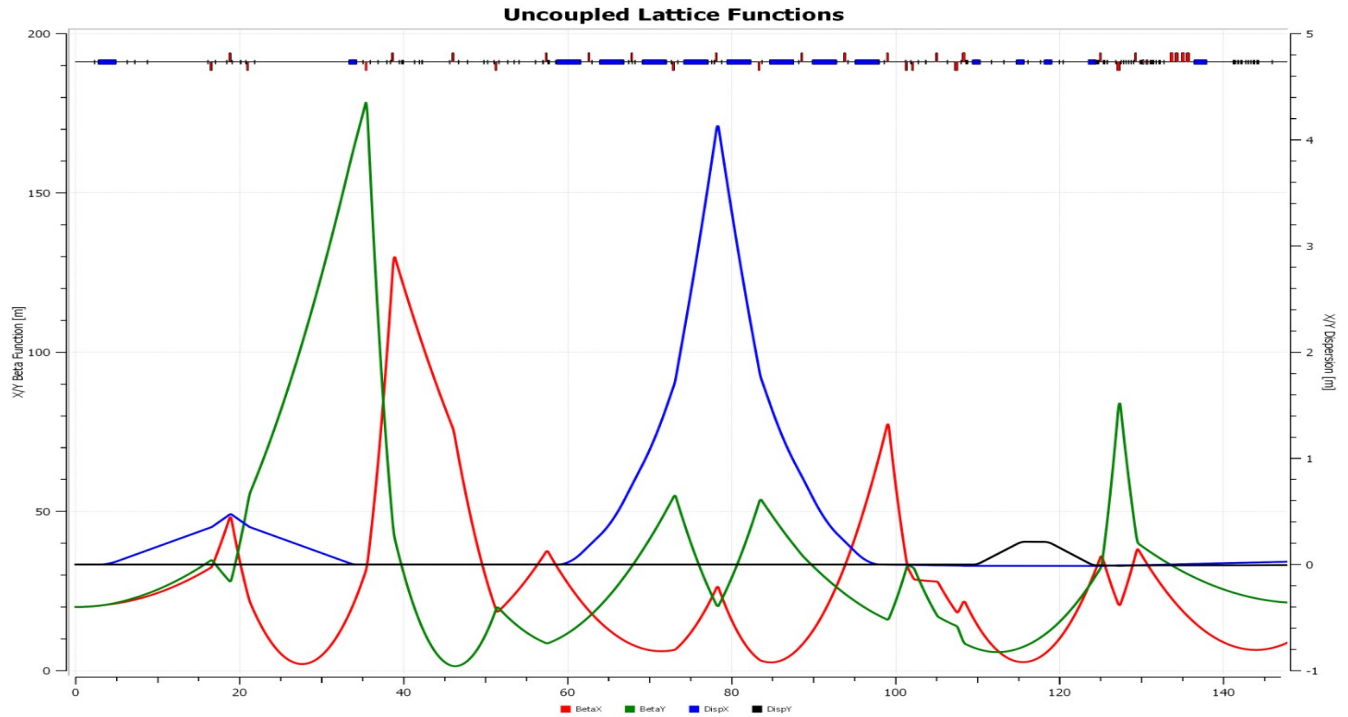


Figure 3. Beta functions and dispersion throughout Hall A line to 32 cm past end of LH2 target.

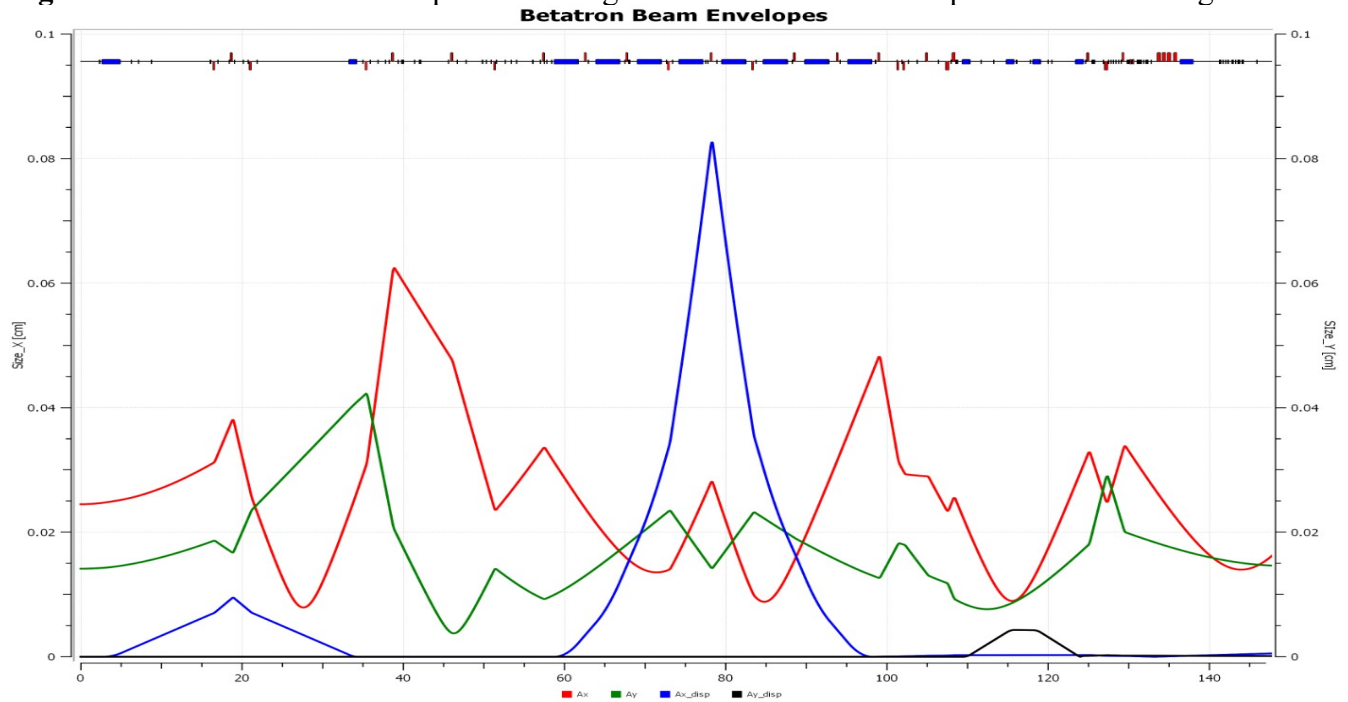


Figure 4. Beam envelopes, 0.5 mm full vertical scale, from end of Hall A transport arc through to 32 cm past end of LH2 target. Horizontal (red) minima are at Compton polarimeter interaction point and at center of MOLLER LH2 target. Horizontal emittance is three times vertical so more focusing is needed. The quadrupole triplet, elements 241, 251 and 265, may be relaxed to move the final minimum either to the pivot or to ~ 4 m beyond it. Beam size would still be within agreed specification at the right hand boundary of Fig. 4 when relaxed to the latter extent. Blue line is envelope due to 4 m dispersion coupled to $2E-4$ momentum spread; horizontal position at the 1C12 BPM, at the peak, is dominated by energy variation.

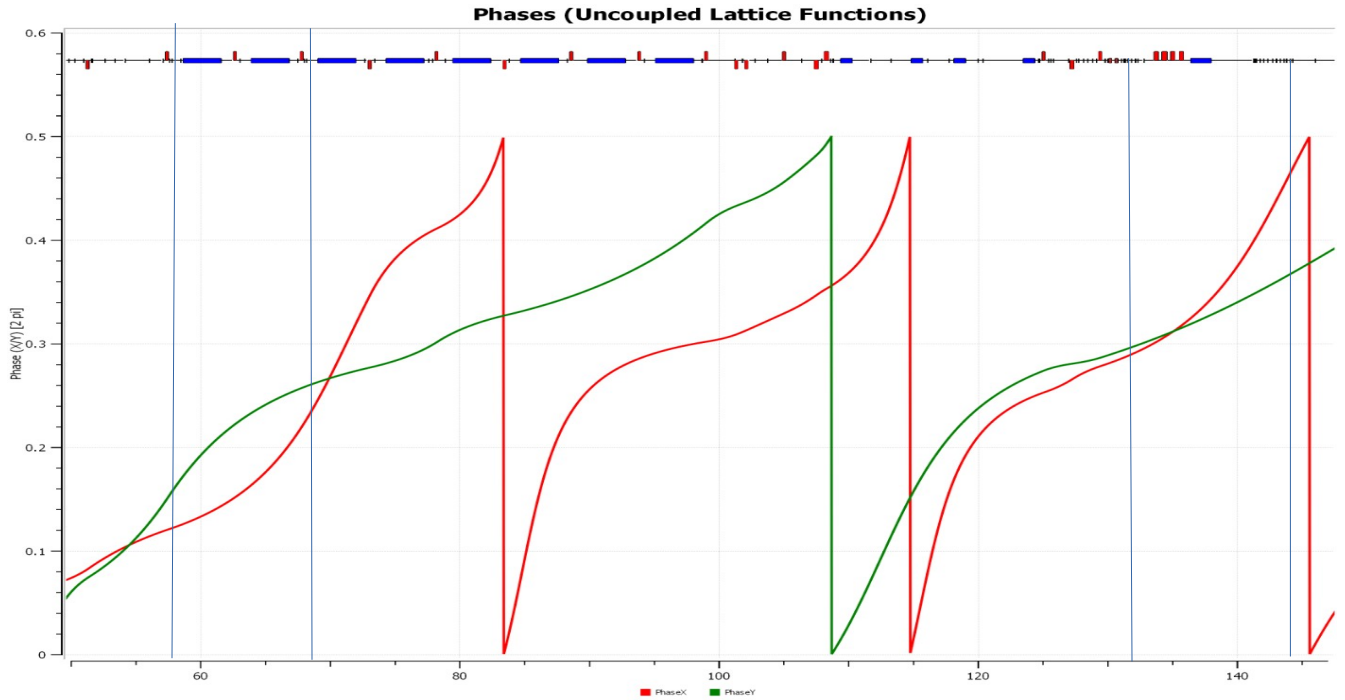


Figure 5. Phase advance from 1C07 quad to 32 cm past end of LH2 target. The two vertical lines at left indicate the position of H/V coils which can be used to excite small position variations to quantify helicity dependent position differences. The two lines at the right are BPMs after all excited magnets. There is adequate but not optimal phase difference between the exciting coils and the BPMs. There are two intermediate BPMs on the right not indicated. The four BPMs in question are elements 275, 287, 301 and 321. Two cavity BPMs are also in this region. If the phase advance proves inadequate one of the coil pairs may be moved during or after the first sixteen week MOLLER run.

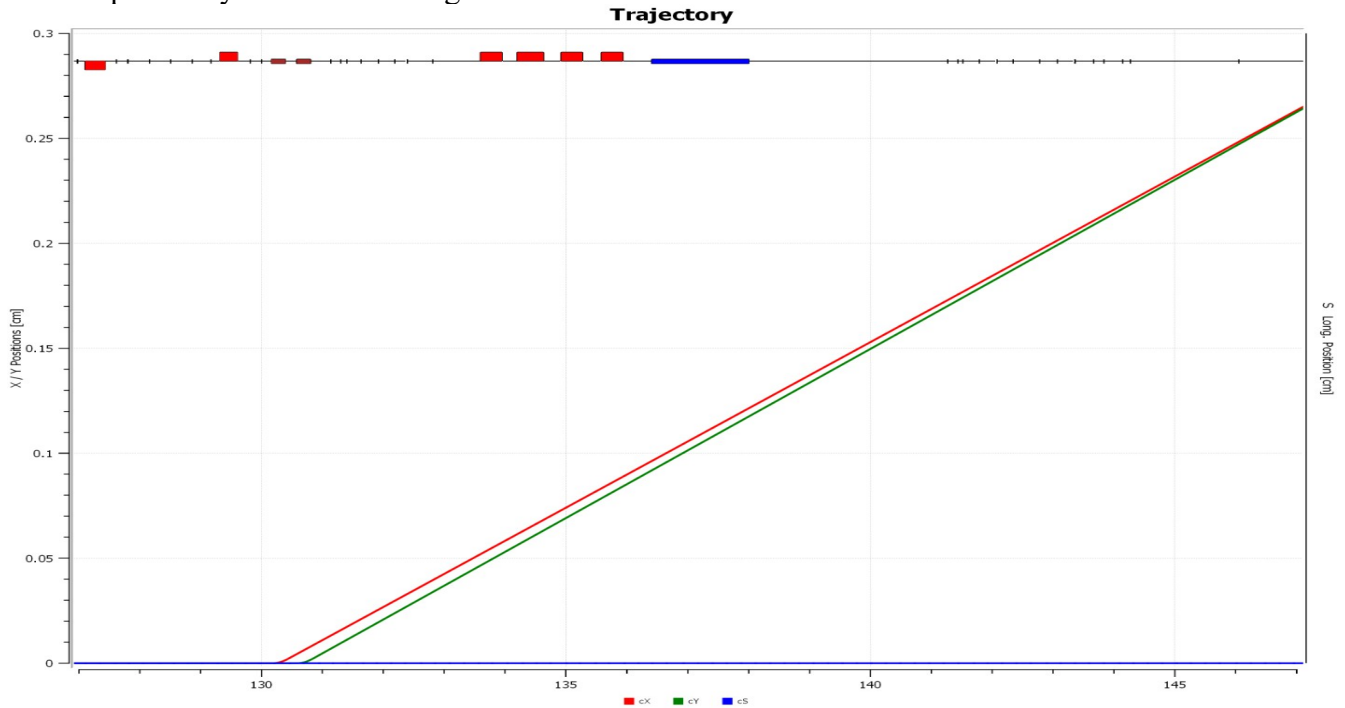


Figure 6. Raster response is linear as all magnets after the raster are degaussed during production running. 81 A in vertical coil, green.

An interim change

The experiments tentatively scheduled for May-December 2022 use a polarized He3 target in a glass cell 600 mm long by 19 mm Inner Diameter (ID). Target cells are described in (x). These are handmade by a university glassblower and are not uniform in dimension. As a result the target cell may be off the beam line axis by a few mm at either end, creating both position and angle offsets. The present beam line, Figures 1 and 2, has inadequate capacity for beam position and angle adjustment. It has been proposed that a portion of the MOLLER beam line rework be done January-April 2022. The third quadrupole girder, elements 262-269, would be replaced by the second existing raster girder so existing raster power supplies can be used. The nA cavity BPM assembly, elements 280-286, would remain in its current location on a long diagnostic girder between the Moller polarimeter and the Pivot. Changes associated with elements 300-328 would not be made at this time. The doublet, elements 241 and 251, does not suffice to create a minimum at the pivot so the Moller polarimeter quads are pressed into service; raster distortion is much less than shown in Figure 2.

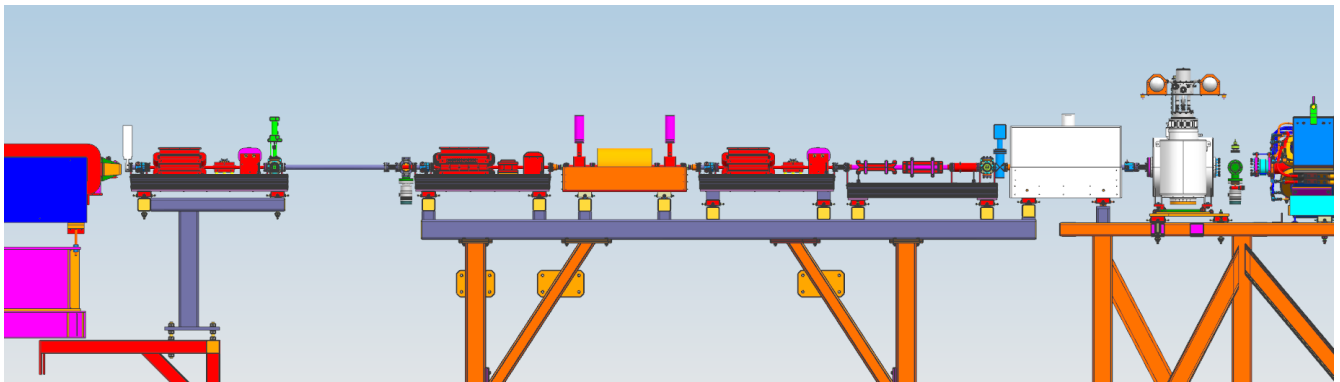


Figure 7. First part MOLLER beam line as described above.

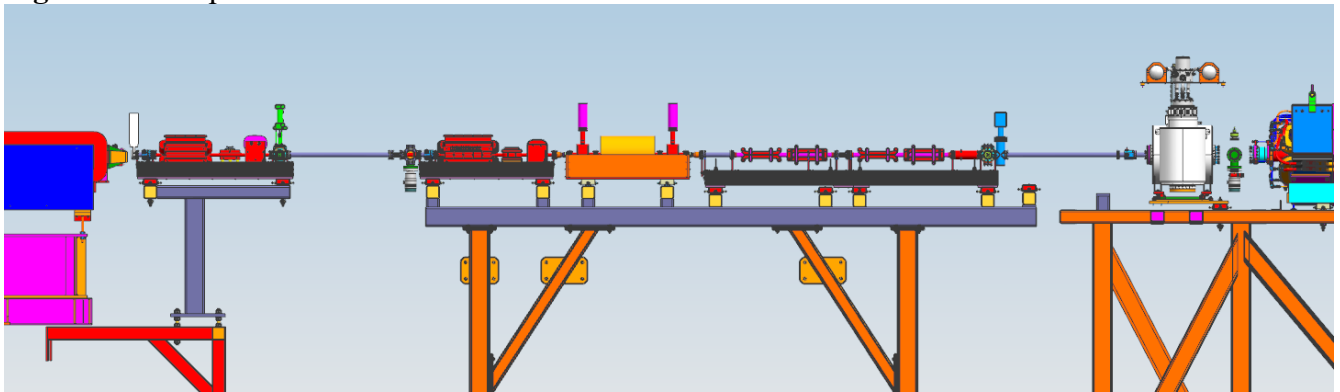


Figure 8. Proposed interim beam line. Third accelerator girder is replaced with existing second set of raster coils. nA BPM (white box) is left on diagnostic girder. Moller polarimeter target is moved upstream 30 cm as requested to improve resolution.

This interim arrangement may be optimized in two manners: one may minimize the spot envelope at the pivot, at the cost of requiring very different currents in the X (41 A) and Y (25 A) rasters to get equal deflection at the pivot, or one may optimize the raster and create a larger spot. In the latter case the currents are 30 A in X and 28 A in Y. This makes it trivial to get a nearly circular raster as desired for the glass target. The existing raster power supplies are rated at 60 A but limited to 50 A for improved reliability. For MOLLER new power supplies are required as the single raster coil per plane requires 81 A. These are not yet available hence the second raster pair will be used.

There is a major improvement in steering capability with the modified design. The existing deck can only manage up to 1.9mm target offset if wanting to come with zero angle or 3.7 mm if not requiring a zero angle. The interim design has a very wide range of X target offset it can accommodate, over 8mm, while also being able to come in with zero angle which is a major advantage for the He3 long target.

In both instances it is assumed one starts with correctors at zero. Obviously if they were not the range may be less. While this is not a problem for the interim design since there is so much headroom, it's an issue with the existing optics. This is pretty much what we have been observing. Around 3mm target offset correction is difficult. Sometimes we rail correctors and have to make suboptimal changes in orbit upstream, compromising the orbit in the Compton polarimeter, in order to get through the offset/tilted target and on to the dump.

With the interim solution, one can implement a “smart knob”, aka a simultaneous software control for multiple correctors. The recipe is: Power MBC1H01H and then set MBC1H02H 60% weaker, set MBD1H04H like 1H02H but with sign reversed. MBD1H04H is on a girder after element 299 in the list above; this girder will be removed in the final beam line.

Figure 9 below shows correction for 1mm target offset in X/Y with the interim solution and correctors H01/H02/H04. It was calculated in ELEGANT and the solution typed into Optim to generate the plot. There are also solutions for which one can decide to use H01/H04 or H02/H04 instead of all three. For MOLLER the three X/Y pairs of correctors (243/245, 253/255, 267/269) will suffice; the 1H04 corrector pair will not exist.

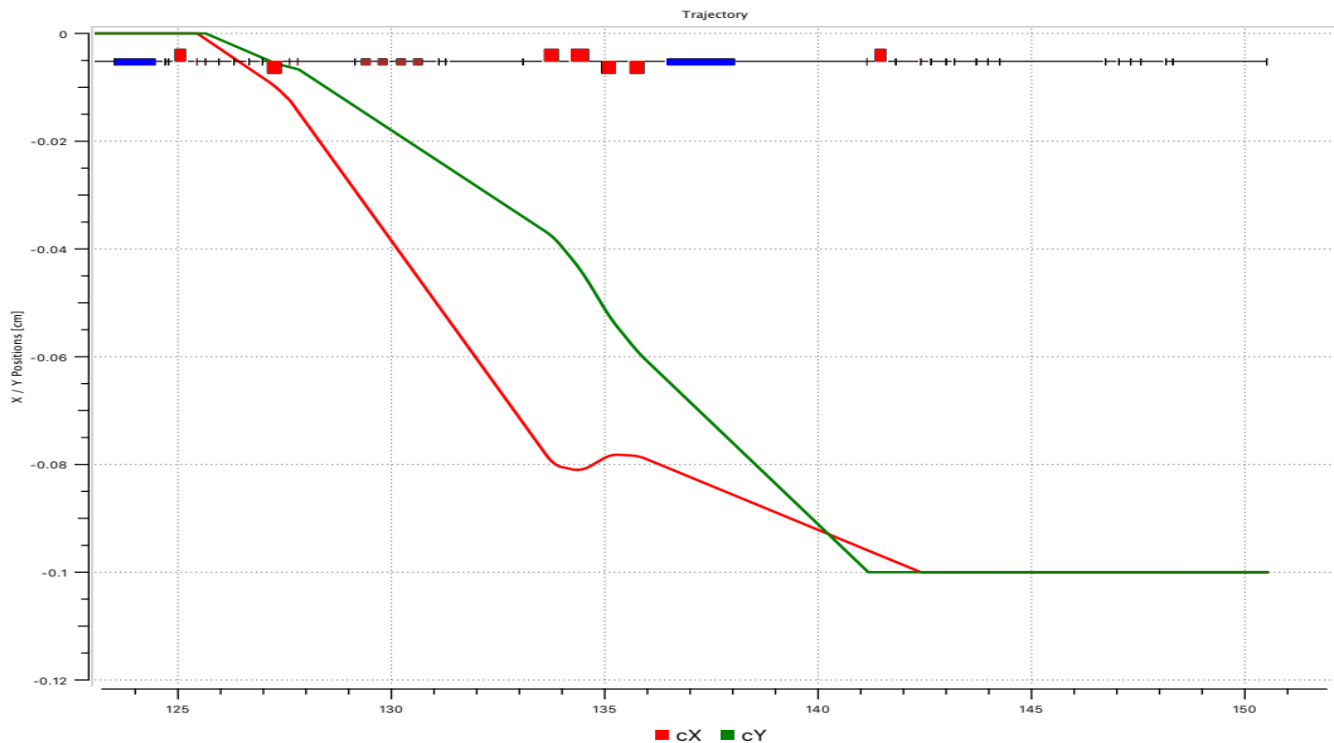


Figure 9. Correction of 1 mm target offsets in both X and Y in the interim optics solution.

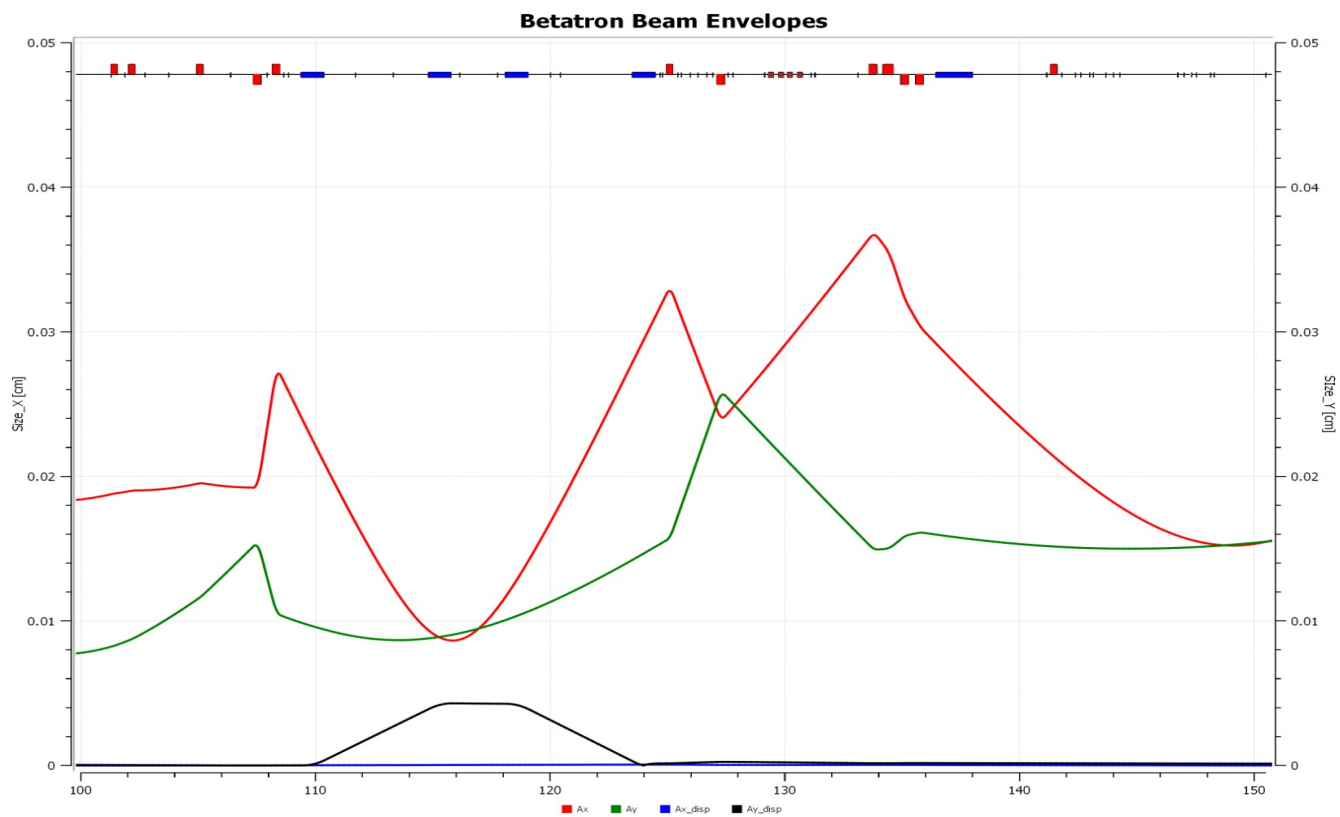


Figure 10. Beam envelopes of interim layout optimized for spot size at pivot (right edge of plot)

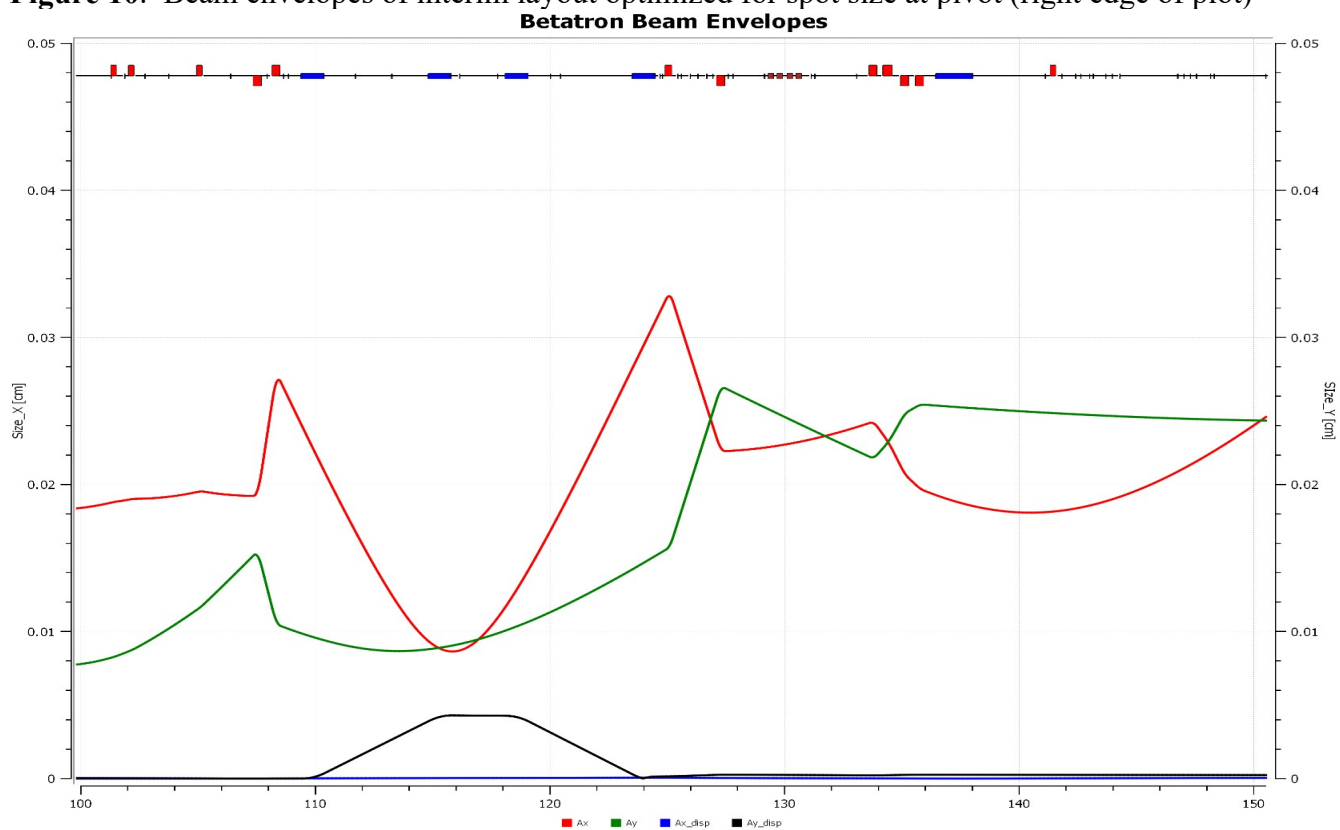


Figure 11. Beam envelopes of interim layout optimized for raster at pivot (right edge of plot). While the spot size is two-thirds larger than in Figure 10, it is still below specification (0.03 cm, 300 microns)

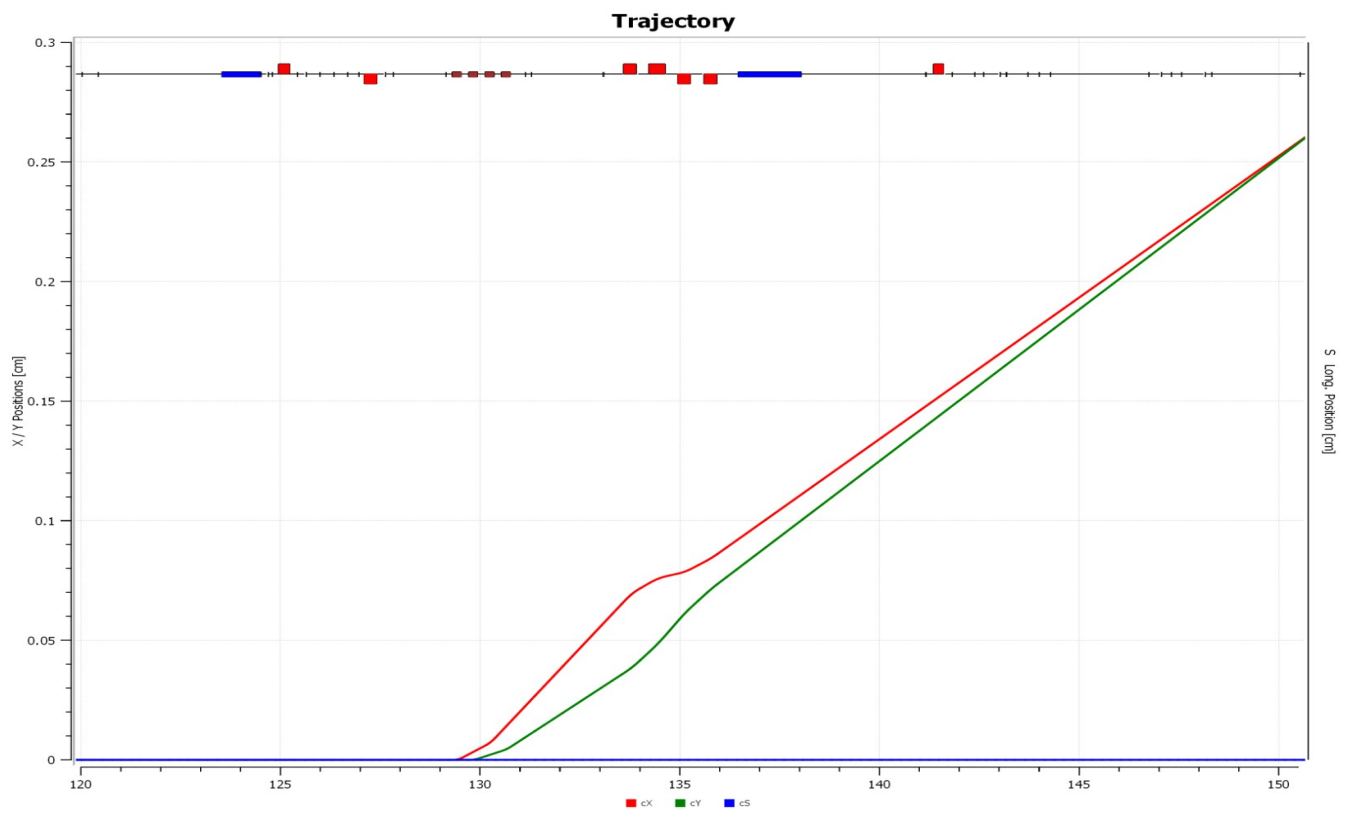


Figure 12. Raster with optics optimized for spot size at pivot, Figure 10.

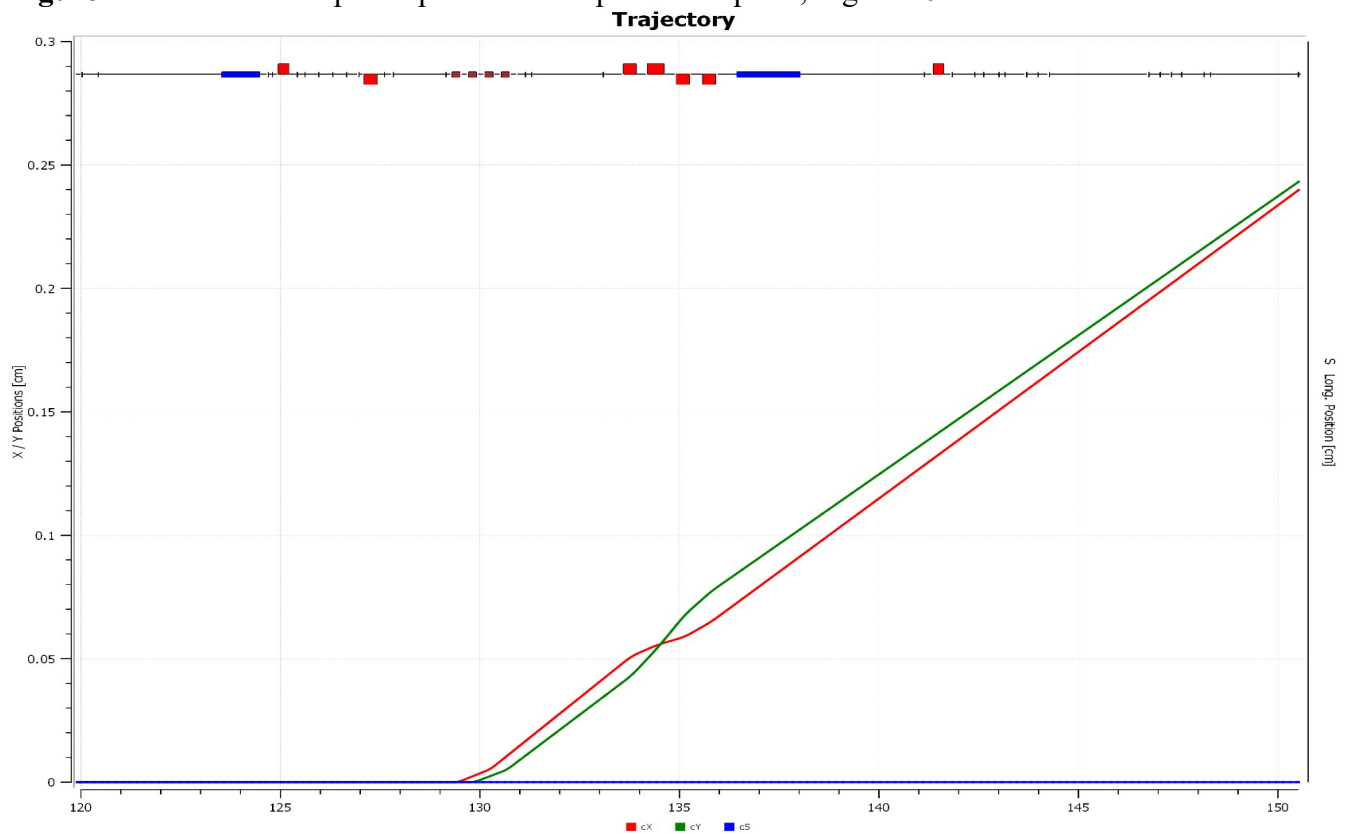


Figure 13 Raster with optics optimized for near-equal coil currents, so a circular raster would be easy to implement. Envelopes in Figure 11.

Conclusions

A beam line based on two decades of experience with parity experiments has been designed. The first half of the line should be installed in the first part of 2022 to gain experience with the altered Moller polarimeter and provide better beam to the experiments scheduled for that year.

References

- 1 V Lebedev, now ported and maintained by J.-F. Ostiguy <https://home.fnal.gov/~ostiguy/OptiM/>
- 2 MOLLER Collaboration: J. Benesch et al. The MOLLER Experiment: An Ultra-Precise Measurement of the Weak Mixing Angle Using Möller Scattering, <https://arxiv.org/abs/1411.4088>
- 3 P. Souder and K. Paschke “Parity violation in electron scattering” *Front.Phys.(Beijing)* 11 (2016) 1, 111301 <https://doi.org/10.1007/s11467-015-0482-0>
- 4 Roger D.Carlini, Willem T.H.van Oers, Mark L.Pitt and Gregory R.Smith, Determination of the Proton’s Weak Charge and Its Constraints on the Standard Model, *Annu.Rev.Nucl.Part.Sci.* 2019.69:191–217 <https://www.annualreviews.org/doi/full/10.1146/annurev-nucl-101918-023633>
- 5 HAPPEX Collaboration, K.A. Aniol et al. New measurement of parity violation in elastic electron - proton scattering and implications for strange form-factors *Phys.Lett.B* 509 (2001) 211-216 <https://arxiv.org/abs/nucl-ex/0006002>
- 6 PREX Collaboration An Accurate Determination of the Neutron Skin Thickness of 208Pb through Parity-Violation in Electron Scattering <https://arxiv.org/abs/2102.10767>
- 7 The Jefferson Lab Qweak Collaboration., Androić, D., Armstrong, D.S. et al. Precision measurement of the weak charge of the proton. *Nature* 557, 207–211 (2018). <https://doi.org/10.1038/s41586-018-0096-0>
- 8 https://moller.jlab.org/DocDB/0006/000630/001/MOLLER_CDR_final_aug_4_2020.pdf
- 9 Poelker et al, in preparation
- 10 K. Unser The parametric current transformer, a beam current monitor developed for LEP AIP Conference Proceedings 252, 266 (1992); <https://doi.org/10.1063/1.42124>
- 11 M. Borland, ”elegant: A Flexible SDDS-Compliant Code for Accelerator Simulation,” Advanced Photon Source LS-287, September 2000.